5
Performance Characteristics of PET Scanners

A major goal of the PET studies is to obtain a good quality and detailed image of an object by the PET scanner, and so it depends on how well the scanner performs in image formation. Several parameters associated with the scanner are critical to good quality image formation, which include spatial resolution, sensitivity, noise, scattered radiations, and contrast. These parameters are interdependent, and if one parameter is improved, one or more of the others are compromised. A description of these parameters is given below.

Spatial Resolution

The *spatial resolution* of a PET scanner is a measure of the ability of the device to faithfully reproduce the image of an object, thus clearly depicting the variations in the distribution of radioactivity in the object. It is empirically defined as the minimum distance between two points in an image that can be detected by a scanner. A number of factors discussed below contribute to the spatial resolution of a PET scanner.

Detector size: One factor that greatly affects the spatial resolution is the intrinsic resolution of the scintillation detectors used in the PET scanner. For multidetector PET scanners, the intrinsic resolution (R_i) is related to the detector size d. R_i is normally given by $d/2$ on the scanner axis at midposition between the two detectors and by d at the face of either detector. Thus it is best at the center of the FOV and deteriorates toward the edge of the FOV. For a 6mm detector, the R_i value is ~3mm at the center of the FOV and ~6mm toward the edge of the FOV. For continuous single detectors, however, the intrinsic resolution depends on the number of photons detected, not on the size of the detector, and is determined by the full width at half maximum of the photopeak.

Positron range: A positron with energy travels a distance in tissue, losing most of its energy and then is annihilated after capturing an electron (Figure 5-1). Thus, the site of β^+ emission differs from the site of annihila-

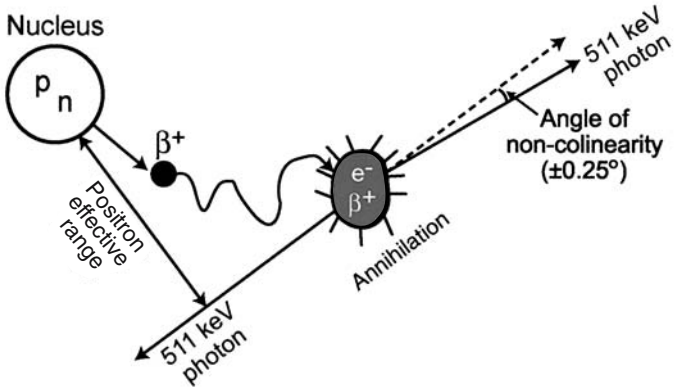

FIGURE 5-1. Positrons travel a distance before annihilation in the absorber and the distance increases with positron energy. Since positrons with different energies travel in zigzag directions, the effective range is the shortest distance between the nucleus and the direction of 511 keV photons. This effective range degrades the spatial resolution of the PET scanner. (Reprinted with the permission of the Cleveland Clinical Foundation.)

tion as shown in Figure 5-1. The distance (range) traveled by the positron increases with its energy, but decreases with the tissue density. Since the positrons are emitted with a spectrum of energy, the positron range is essentially an effective range, which is given by the shortest (perpendicular) distance from the emitting nucleus to the positron annihilation line. The effective positron ranges in water for ^{18}F ($E_{\beta+,max}$ = 0.64 MeV) and ^{82}Rb ($E_{\beta+,max}$ = 3.35 MeV) are 2.2 mm and 15.5 mm, respectively (Table 1.2). Since coincidence detection is related to the location of annihilation and not to the location of β^+ emission, an error (R_p) occurs in the localization of true position of the positron emission thus resulting in the degradation of spatial resolution. This contribution (R_p) to the overall spatial resolution is determined from the FWHM of the positron count distribution, which turns out to be 0.2 mm and 2.6 mm for ^{18}F and ^{82}Rb respectively (Tarantola et al., 2003).

Non-colinearity: Another factor of concern is the non-colinearity that arises from the deviation of the two annihilation photons from the exact 180° position. That is, two 511 keV photons are not emitted at exactly 180° after the annihilation process (Figure 5-2), because of some small residual momentum of the positron at the end of the positron range. The maximum deviation from the 180° direction is ±0.25° (i.e., 0.5° FWHM). Thus, the observed LOR between the two detectors does not intersect the point of annihilation, but is somewhat displaced from it, as illustrated in Figure 5-2. This error (R_a) degrades the spatial resolution of the scanner and deteriorates with the distance between the two detectors. If D is the distance in cm between the two detectors (i.e., detector ring diameter), then R_a can be calculated from the point-spread-function as follows:

$$R_a = 0.0022D \tag{5.1}$$

The contribution from non-colinearity worsens with larger diameter of the ring, and it amounts to 1.8 to 2 mm for currently available 80-cm to 90-cm PET scanners.

Reconstruction method used: Choice of filters with a selected cut-off frequency in the filtered backprojection reconstruction method may introduce additional degradation of the spatial resolution of the scanner. For example, a filter with a too high cut-off value introduces noise and thus degrades spatial resolution. An error (K_r) due to the reconstruction technique is usually a factor of 1.2 to 1.5 depending on the method (Huesman, 1977).

Localization of detector: The use of block detectors instead of single detectors causes an error (R_ℓ) in the localization of the detector by X, Y analysis and it may amount to 2.2 mm for BGO detectors (Moses and Derenzo, 1993). However, it can be considerably minimized by using better light output scintillators, such as LSO.

Combining the above factors, the overall spatial resolution R_t of a PET scanner is given by

$$R_t = K_r \times \sqrt{R_i^2 + R_p^2 + R_a^2 + R_\ell^2} \tag{5.2}$$

In whole-body scanners, the detector elements are normally large and therefore, $R_i(d$ or $d/2)$ is large so that the contribution of R_p is negligible

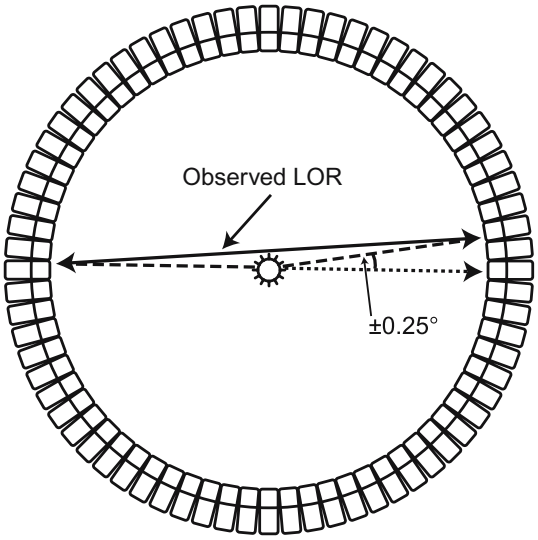

FIGURE 5-2. Non-colinearity of 511 keV annihilation photons. Because there is some residual momentum associated with the positron, the two annihilation photons are not emitted exactly at 180°, but at a slight deviation from 180°. Two detectors detect these photons in a straight line, which is slightly deviated from the original annihilation line. The maximum deviation is ±0.25°. (Reprinted with the permission of the Cleveland Clinical Foundation.)

for ^{18}F-FDG ($E_{\beta+,\max} = 0.64\,\text{MeV}$) whole body imaging. For ^{18}F-FDG studies using a 90-cm diameter PET scanner with 6 mm detectors, $R_a \sim 2\,\text{mm}$, and assuming $R_b = 0$, $R_e = 2.2\,\text{mm}$ and $K_r = 1.5$, $R_t = 1.5 \times \sqrt{3^2 + (2.2)^2 + 2^2}$ $= 6.3\,\text{mm}$ at the center and $R_t = 1.5 \times \sqrt{6^2 + (2.2)^2 + 2^2} = 10.0\,\text{mm}$ at the face of the detector.However, the contribution of R_p may be appreciable for high-energy positron emitters (e.g., ^{82}Rb; $E_{\beta+,\max} = 3.35\,\text{MeV}$) and small animal PET scanners (e.g., microPET system) having smaller detectors.

The detailed method of measuring the spatial resolution of a PET scanner is given later in this chapter. The spatial resolutions of PET scanners from different manufacturers are given in Table 5.1.

Sensitivity

The sensitivity of a PET scanner is defined as the number of counts per unit time detected by the device for each unit of activity present in a source. It is normally expressed in counts per second per microcurie (or megabecquerel) (*cps*/μ*Ci* or *cps*/*MBq*). Sensitivity depends on the geometric efficiency, detection efficiency, PHA window settings, and the dead time of the system. The detection efficiency of a detector depends on the scintillation decay time, density, atomic number, and thickness of the detector material that have been discussed in Chapter 2. Also, the effect of PHA window setting on detection efficiency has been discussed in Chapter 2. The effect of the dead time on detection efficiency has been described in Chapter 3. In the section below, only the effects of geometric efficiency and other related factors will be discussed.

The geometric efficiency of a PET scanner is defined by the solid angle projected by the source of activity at the detector. The geometric factor depends on the distance between the source and the detector, the diameter of the ring and the number of detectors in the ring. Increasing the distance between the detector and the source reduces the solid angle and thus decreases the geometric efficiency of the scanner and vice versa. Increasing the diameter of the ring decreases the solid angle subtended by the source at the detector, thus reducing the geometric efficiency and in turn the sensitivity. Also the sensitivity increases with increasing number of rings in the scanner.

Based on the above factors discussed, the sensitivity S of a single ring PET scanner can be expressed as (Budinger, 1998):

$$S = \frac{A \cdot \varepsilon^2 \cdot e^{-\mu t} \cdot 3.7 \times 10^4}{4\pi r^2} (cps/\mu Ci) \tag{5.3}$$

where A = detector area seen by a point source to be imaged, ε = detector's efficiency, μ is the linear attenuation coefficient of 511 keV photons in the detector material, t is the thickness of the detector, and r is the radius of the detector ring.

TABLE 5.1. Performance data of different PET scanners[1].

Performance	ADVANCE/ ADVANCE Nxi (General Electric)	ECAT ACCEL (CTI-Siemens)	ECAT EXACT HR+ (CTI-Siemens)	ECAT EXACT (CTI-Siemens)	ECAT ART (CTI-Siemens)	C-PET (Philips-ADAC)	ALLEGRO (Philips-ADAC)
Transaxial resolution							
FWHM (mm) at 1 cm		6.2 (2D)	4.6 (2D)				
	4.8 (2D/3D)	6.3 (3D)*	4.5 (3D)*	6.0 (2D/3D)	6.2	5.0*	4.8*
FWHM (mm) at 10 cm		6.7 (2D)	5.4 (2D)				
	5.4 (2D/3D)	7.4 (3D)*	5.6 (3D)*	6.7 (2D/3D)	6.9	6.4*	5.9*
Axial resolution							
FWHM (mm) at 0 cm	4.0 (2D)	4.3 (2D)	4.2 (2D)	4.5 (2D)			
	4.7 (3D)	5.8 (3D)*	4.2 (3D)*	4.6 (3D)	4.9	5.5*	5.4*
FWHM (mm) at 10 cm	5.4 (2D)	6.0 (2D)	5.0 (2D)	5.9 (2D)			
	6.3 (3D)	7.1 (3D)*	5.7 (3D)*	6.5 (3D)	6.6	5.9*	6.5*
System sensitivity	5.4 (2D)†	5.4 (2D)	5.4 (2D)	4.9 (2D)			
(net trues) (cps/Bq/mL)	31.0 (3D)‡	27.0 (3D)	24.3 (3D)	21.2 (3D)	7.3	12.1*	19.0*
Scatter fraction (%)	10 (2D)	16 (2D)	17 (2D)	16 (2D)			
	35 (3D)	36 (3D)	36 (3D)	36 (3D)	36	25	25

[1] Reprinted with permission of the Society of Nuclear Medicine from: Tarantola et al PET Instrumentation and Reconstruction Algorithms in Whole-body Applications. *J Nuc Med.* 2003;44:756–769.

* Assessed according to NEMA NU 2–2001, National Electrical Manufacturers Association; 2001.

† Measured at 300-keV LLD in high sensitivity mode.

‡ Measured at 300-keV LLD.

All other parameters were measured following NEMA NU 2–1994, National Electrical Manufacturers Association, 1994.

Equation (5.3) is valid for a point source at the center of a single ring scanner. For an extended source at the center of such scanners, it has been shown that the geometric efficiency is approximated as $w/2r$, where w is the axial width of the detector element and r is the radius of the ring (Cherry et al., 2003). Thus the sensitivity of a scanner is highest at the center of the axial FOV and gradually decreases toward the periphery. In typical PET scanners, there are also multiple rings and each detector is connected in coincidence with as many as half the number of detectors on the opposite side in the same ring as well as with detectors in other rings.Thus the sensitivity of multiring scanners will increase with the number of rings.

Note that the sensitivity of a PET scanner increases as the square of the detector efficiency, which depends on the scintillation decay time and atomic number of the detector. This is why LSO and GSO detectors are preferred to NaI(Tl) or BGO detectors (see Table 2.1). In 2-D acquisitions, system sensitivity is compromised because of the use of septa between detector rings, whereas these septa are retracted or absent in 3-D acquisition, and hence the sensitivity is increased by a factor of 4 to 8. However, in 3-D mode, random and scatter coincidences increase significantly, the scatter fraction being 30% to 40% compared to 15% to 20% in 2-D mode. The overall sensitivities of PET scanners for a small-volume source of activity are about 0.2% to 0.5% for 2-D acquisition and about 2% to 10% for 3-D acquisition, compared to 0.01% to 0.03% for SPECT studies (Cherry et al., 2003). The greater sensitivity of the PET scanner results from the absence of collimators in data acquisition.

Sensitivity is also given by volume sensitivity expressed in units of $k$cps/μCi/cc or cps/Bq/cc. It is determined by acquiring data in all projections for a given duration from a volume of activity (uniformly mixed) and dividing the total counts by the duration of counting and by the concentration of the activity in the source. Manufacturers normally use this unit as a specification for the PET scanners. The detailed method of determining volume sensitivity is described under acceptance tests in this chapter. The volume sensitivities of PET scanners from different manufacturers are given in Table 5.1.

Noise Equivalent Count Rate

Image noise is the random variation in pixel counts across the image and is given by $(1/\sqrt{N}) \times 100$, whose N is the counts in the pixel. It can be reduced by increasing the total counts in the image. More counts can be obtained by imaging for a longer period, injecting more radiopharmaceutical, or improving the detection efficiency of the scanner. All these factors are limited by various conditions, e.g., too much more activity cannot be administered because of increased radiation dose to the patient, random coincidence counts, and dead time loss. Imaging for a longer period may be uncomfortable to the patient and improving the detection efficiency may be limited by the design of the imaging device.

The image noise is characterized by a parameter called the *noise equivalent count rate* (*NECR*) which is given by

$$NECR = \frac{T^2}{T + S + R} \tag{5.4}$$

where T, R, and S are the true, random, and scatter coincidence count rates, respectively. This value is obtained by using a 20cm cylindrical phantom of uniform activity placed at the center of the FOV and measuring prompt coincidence counts. Scatter and random events are measured according to methods described later in this chapter. The true events (T) are determined by subtracting scatter (S) and random (R) events from the prompt events. From the knowledge of T, R and S, the *NECR* is calculated by Eq. (5.4). The *NECR* is proportional to the signal-to-noise (*SNR*) ratio in the final reconstructed images and, therefore, serves as a good parameter to compare the performances of different PET scanners. The 3-D method has a higher *NECR* at low activity. However, the peak *NECR* in the 2-D mode is higher than the peak *NECR* in the 3-D mode at higher activity. Image noise can be minimized by maximizing *NECR*.

Another type of image noise arises from nonrandom or systematic addition of counts due to imaging devices or procedural artifacts. For example, bladder uptake of ^{18}F-FDG may obscure the lesions in the pelvic area. Various "streak" type artifacts introduced during reconstruction may be present as noise in the image.

Scatter Fraction

The scatter fraction (*SF*) is another parameter that is often used to compare the performances of different PET scanners. It is given by

$$SF = \frac{C_S}{C_p} \tag{5.5}$$

where C_s and C_p are the scattered and prompt count rates. The lower the SF value, the better the performance of a scanner and better the quality of images. The method of determining SF is given later in this chapter. Comparative *SF* values for different PET scanners are given in Table 5.1.

Contrast

Contrast of an image arises from the relative variations in count densities between adjacent areas in the image of an object. Contrast (C) gives a measure of the detectability of an abnormality relative to normal tissue and is expressed as

$$C = \frac{A - B}{A} \tag{5.6}$$

where A and B are the count densities recorded in the normal and abnormal tissues, respectively.

Several factors affect the contrast of an image, namely: count density, scattered radiations, type of film, size of the lesion, and patient motion. Each contributes to the contrast to a varying degree. These factors are briefly discussed here.

Statistical variations of the count rates give rise to noise that increases with decreasing information density or count density (counts/cm^2), and are given by $(1/\sqrt{N}) \times 100$, where N is the count density. For a given image, a minimum number of counts are needed for a reasonable image contrast. Even with adequate spatial resolution of the scanner, lack of sufficient counts may give rise to poor contrast due to increased noise, so much so that lesions may be missed. This count density in a given tissue depends on the administered dosage of the radiopharmaceutical, uptake by the tissue, length of scanning, and the detection efficiency of the scanner. The activity of a dosage, scanning for a longer period, and the efficiency of a scanner are optimally limited, as discussed above under Noise Equivalent Count Rate. The uptake of the tracer depends on the pathophysiology of the tissue in question. Optimum values for a procedure are obtained from the compromise of these factors.

Background in the image increases with scattered radiations and thus adds to degradation of the image contrast. Maximum scatter radiations arise from the patient. Narrow PHA window settings can reduce the scatter radiations, but at the same time the counting efficiency is reduced.

Image contrast to delineate a lesion depends on its size relative to system resolution and its surrounding background. Unless a minimum size of a lesion develops larger than system resolution, contrast may not be sufficient to appreciate the lesion, even at higher count density. The effect of lesion size depends on the background activity surrounding it and on whether it is a "cold" or "hot" lesion. A relatively small-size "hot" lesion is easily well contrasted against a lower background, whereas a small-size "cold" lesion may be missed against the surrounding tissue of increased activities.

Film contrast is a component of overall image contrast and depends on the type of film used. The density response characteristics of x-ray films are superior to those of Polaroid films and provide the greatest film contrast, thus adding to the overall contrast. Developing and processing of exposed films may add artifacts to the image and, therefore, should be carried out carefully.

Patient motion during imaging reduces the image contrast. This primarily results from the overlapping of normal and abnormal areas due to movement of the organ. It is partly alleviated by restraining the patient or by having him in a comfortable position. Artifacts due to heart motion can

be reduced by using the gated technique. Similarly, breath holding may improve the thoracic images.

Quality Control of PET Scanners

In the image formation of an object using PET scanners, several parameters related to the scanners play a very important role. To ensure high quality of images, several quality control tests must be performed routinely on the scanner. The frequency of these tests is either daily or weekly, or even at a longer interval depending on the type of parameter to be evaluated.

Daily Quality Control Tests

Sinogram (uniformity) check: Sinograms are obtained daily using a long-lived ^{68}Ge or ^{137}Cs source mounted by brackets on the gantry and rotating it around the scan field without any object in the scanner. It can also be done by using a standard phantom containing a positron emitter at the center of the scanner. All detectors are uniformly exposed to radiations to produce homogeneous detector response and hence a uniform sinogram. A malfunctioning detector pair will appear as a streak in the sinogram.

Typically, the daily acquired blank sinogram is compared with a reference blank sinogram obtained during the last setup of the scanner. The difference between the two sinograms is characterized by the value of the so-called average variance, which is a sensitive indicator of various detector problems. It is expressed by the square sum of the differences of the relative crystal efficiencies between the two scans weighted by the inverse variances of the differences. The sum divided by the total number of crystals is the average variance. If the average variance exceeds 2.5, recalibration of the PET scanner is recommended, whereas for values higher than 5.0, the manufacturer's service is warranted (Buchert et al., 1999). In Figure 3-3, the average variance between the two scans is 1.1, indicating all detectors are working properly.

Weekly Quality Control Tests

In the weekly protocol, system calibration and plane efficiency are performed by using a uniform standard phantom filled with radioactivity, and normalization is carried out by using a long-lived radionuclide rotating around the field of view or a standard phantom with radioactivity placed at the centre of the scanner.

System Calibration: A system calibration scan is obtained by placing the standard phantom containing a positron emitter in a phantom holder at the center of the FOV for uniform attenuation and exposure. The reconstructed

images are checked for any nonuniformity. A bad detector indicates a decreased activity in the image, and warrants the adjustment of PM tube voltage and the discriminator settings of PHA.

Plane Efficiency: The plane efficiency test compares the variations in uniformity of images between planes. After the system calibration is completed, the plane efficiency scans are acquired by keeping the standard phantom at the center of the field. The scans are compared, and interplane efficiency variations are corrected by the computer using multiplication factors to average the plane's responses, which results in uniform images. Note that system calibration and plane efficiency need not be done weekly if the daily quality control data are within the acceptable limits.

Normalization: As discussed in Chapter 3, normalization corrects for nonuniformities in images due to variations in the gain of PM tubes, location of the detector in the block and the physical variation of the detector. This test is carried out by using a rotating rod source of a long-lived radionuclide (normally ^{68}Ge) mounted on the gantry parallel to the axis of the scanner or using a standard phantom containing a positron-emitter at the center of the scanner. The activity used in the source is usually low to avoid dead time loss. Data are acquired in the absence of any object in the FOV. This exposes all detectors uniformly. The multiplication factor for each detector is calculated by dividing the average of counts of all detector pairs by each individual detector pair count (i.e., along the LOR) (Eq. 3.3). These factors are saved and later applied to the corresponding detector pairs in the acquired emission data of the patient (Eq. 3.4). Normalization factors normally are determined weekly or monthly. To have better statistical accuracy in individual detector pair counts, several hours of counting is necessary depending on the type of scanner, and therefore, overnight acquisition of data is often made.

Acceptance Tests

Acceptance tests are a battery of quality control tests performed to verify various parameters specified by the manufacturer for a PET scanner. These are essentially carried out soon after a PET scanner is installed in order to establish the compliance of specifications of the device. The most common and important specifications are transverse radial, transverse tangential, and axial resolutions; sensitivity; scatter fraction; and count rate performance. It is essential to have a standard for performing these tests so that a meaningful comparison of scanners from different manufacturers can be made.

In 1991, the Society of Nuclear Medicine (SNM) established a set of standards for these tests for PET scanners (Karp et al., 1991). Afterward, in 1994, the National Electrical Manufacturers Association (NEMA) published a document, NU 2-1994, recommending improved standards for performing these tests, using a 20×19 cm phantom (NEMA, 1994)

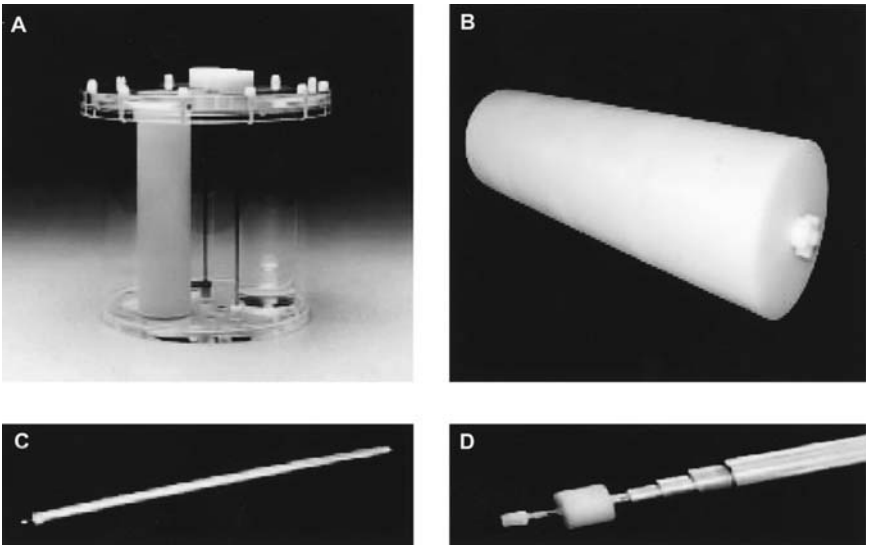

FIGURE 5-3. NEMA phantoms for PET performance tests. (A) This phantom is used for evaluation of count rate, uniformity, scatter fraction, and attenuation according to the NEMA NU 2-1994 standard, (B) This phantom is used for measuring scatter fraction, dead time, and random counts in PET studies using the NEMA NU 2-2001 standard, (C) Line source phantom consisting of 6 concentric aluminum tubes to measure the sensitivity of PET scanners, (D) Close up end of phantom (C). (Courtesy of Data Spectrum Corporation, Hillborough, NC.)

(Figure 5-3A). This phantom is useful for earlier scanners, in which the axial FOV is less than 17 cm and data are acquired in 2-D mode, because of the use of septa. Modern whole-body PET scanners have axial FOVs as large as 25 cm, and employ 3-D data acquisition in the absence of septa. The coincidence gamma cameras have typical FOVs of 30 to 40 cm. Because of larger FOVs and high count rates in 3-D mode, the NU 2-1994 phantom may not be accurately applied for some tests in some scanners, and a new NU 2-2001 standard has been published by NEMA in 2001 (NEMA, 2001). The phantom used measures 70 cm long compared to 19 cm for the NU 2-1994 phantom (Figure 5-3B). While the NU 2-1994 phantom is still used for some parameters and in earlier scanners, the NU 2-2001 standard is employed to measure several parameters (e.g., sensitivity) in modern whole-body scanners and coincidence gamma cameras. Daube-Witherspoon et al. (2002) have reported the methods of performing these tests based on the NEMA NU 2-2001 standard. The following is a brief description of these tests for some important parameters based on this article and the methods of NEMA NU 2-2001 standard. One should refer to Daube-Witherspoon et al. (2002), NU 2-1994 and NU 2-2001 standards of NEMA for details. Various pertinent parameters for PET scanners from different manufacturers are given in Table 5.1. Note that the table contains data based on both standards.

Spatial Resolution

The spatial resolution of a PET scanner is determined by the full width at half maximum (FWHM) of point-spread-functions (PSF) obtained from measurement of activity distribution from a point source. The spatial resolution can be transverse radial, transverse tangential, and axial, and these values are given in Table 5.1 for scanners from different manufacturers.

The spatial resolution is measured by using six point sources of ^{18}F activity contained in glass capillary in a small volume of less than 1 cc (Daube-Witherspoon et al., 2002). For axial resolutions, two positions—at the center of the axial FOV and at 1/4th of axial FOV—are chosen (Figure 5-4). At each axial position, three point sources are placed at $x = 0$, $y = 1$ cm (to avoid too many sampling of LORs), x = 10 cm, y = 0, and x = 0, y = 10 cm. Data are collected for all six positions and from reconstructed image data, PSFs are obtained in X, Y, and Z directions for each point source at each axial position. The FWHMs are determined from the width at 50% of the peak of each PSF, totaling 18 in number. Related FWHMs are combined and then averaged for the two axial positions to give the transverse radial, transverse tangential and axial resolutions. Transverse resolution worsens as the source is moved away from the center of the FOV (Figure 5-5), i.e., the resolution is best at the center and deteriorates toward the periphery of the scanner.

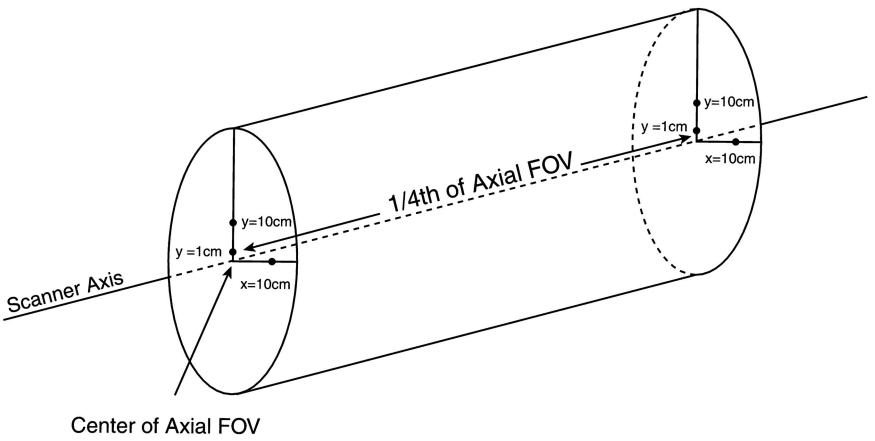

FIGURE 5-4. Arrangement of 6-point sources in the measurement of spatial resolution. Three sources are positioned at the center of the axial FOV and 3 sources are positioned at 1/4th of the axial FOB away from the center. At each position, sources are placed on the positions indicated in a transverse plane perpendicular to the scanner axis. (Reprinted with the permission of the Cleveland Clinic Foundation.)

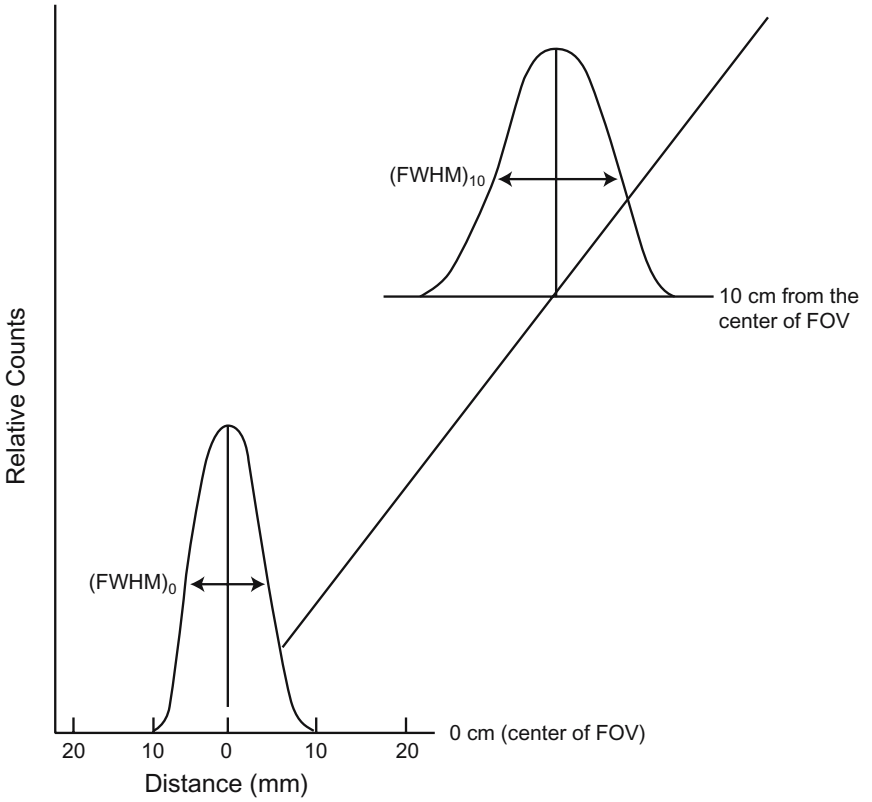

FIGURE 5-5. Point spread functions (PSF) at 0 and 10cm from the center of the FOV. The transverse resolution (FWHM) is best at the center and worsens both radially and axially across the FOV. (Reprinted with the permission of the Cleveland Clinic Foundation.)

Scatter Fraction

Scattered radiations add noise to the reconstructed image, and the contribution varies with different PET scanners. Normally the test is performed with a very high activity source counted over a period of time, from which high activity data are used for determination of random events and count losses (see later) and low activity data for scatter fraction. A narrow line source made of 70cm long plastic tubing and filled with high activity of ^{18}F is inserted into a 70×20cm cylindrical polyethylene phantom through an axial hole made at a radial distance of 4.5cm and parallel to the central axis of the phantom (Figure 5-3B). The phantom is placed at the center both axially and radially on the scan table such that the source is closest to the patient table, since the line source and the bed position affect the measured results.

Data are acquired over time until dead time count losses and random events are reduced to less than 1% of the true rates. These low activity data are used to form sinograms for calculation of scatter fractions. A sinogram profile of an extended diameter of 24 cm (4 cm larger than the phantom) is used, because the FOV varies with different scanners. Each projection in the sinogram is shifted so that the peak of the projection is aligned with the center of the sinogram (line source image). This produces a sum projection with a counts density distribution around the maximum counts (peak) at the center of the sinogram (NEMA, 2001). It is arbitrarily assumed that all true events including some scatter lie within a 4-cm-wide strip centered in each sinogram of the line source and there are no true events but scatter events beyond ±2 cm from the center of the sinogram. Thus the total counts C_T is the area under the peak that includes true events and scatter events plus scatter events outside the peak. The scattered events under the peak are then estimated by taking the average of the pixel counts at ±2 cm positions from the center and multiplying the average with the number of pixels along the 4-cm strip. The product is added to the counts in pixels outside the peak to give total scatter events for the slice. For better statistical accuracy, several acquisitions are made, and the total counts and scatter counts of the corresponding slices are separately summed for all acquisitions. Note that the total counts, C_T, has no or negligible random counts. If C_S and C_T are the scatter counts and total counts, respectively, for a slice, then the scatter fraction SF_i for the slice is given by Eq. (5.5) as

$$SF_i = C_S / C_T \tag{5.7}$$

The system scatter fraction SF is calculated from the weighted average of the SF_i values of all slices. The true count rate R_{true} for a slice is calculated as

$$R_{true} = (C_T - C_S)/t \tag{5.8}$$

where t is the total time of acquisition.

Sensitivity

The sensitivity is a measure of counting efficiency of a PET scanner and is expressed in count rate (normally, cps) per unit activity concentration (normally, MBq or μCi per cc). The NU 2-1994 standard using the 20 × 19 cm phantom underestimates the sensitivity of larger whole-body scanners. The phantom recommended in the NU 2-2001 standard also is too large (70 × 20 cm) and impractical to fill and handle radioactivity. Instead, a 70-cm-long plastic tube filled with a known amount (A_{cal}) of a radionuclide is used (Figure 5-3C, D) (Daube-Whitherspoon et al., 2002). The level of activity is kept low so as to have negligible random events and count loss. The source is encased in metal sleeves of various thicknesses and suspended at the

center of the transverse FOV in parallel to the axis of the scanner in such a way that the supporting unit stays outside the FOV.

Successive data are collected in sinograms using five metal sleeves and an energy window of 410 to 665 keV. Duration of acquisition and total counts in the slice are recorded for each sleeve, from which the count rate is calculated. The count rates are corrected for decay to the time of calibration of radioactivity and then summed for all slices to give the total count rate for each sleeve. Next, the natural logarithm of the measured total count rate (R_i) is plotted as a function of sleeve thickness. After fitting of the data by linear regression, the extrapolated count rate (R_0) with no metal sleeve (attenuation correction) is obtained. The system sensitivity S is given by

$$S = R_0 / A_{cal} \tag{5.9}$$

where A_{cal} is the calibrated activity added to the tubing. The sensitivity is given in either *kcps*/*μCi*/*cc* or *cps*/*MBq*/*cc*. The measurement of sensitivity is repeated with the source placed radially at 10 cm from the center of the transverse FOV. The system sensitivity of commercial PET scanners for 0 cm position is given in Table 5.1.

Count Rate Losses and Random Coincidences

To characterize the count rate behavior of a PET scanner at high activity, random events, noise equivalent count rate, and dead time loss are determined as a function of activity. The activity source is the same as described above under Scatter Fraction in this chapter. A high activity source of ^{18}F is used to acquire the sinogram and data are collected using an energy window of 410 to 665 keV until the activity level is low enough to consider random events and dead time count losses to be negligible. The total counts are obtained from each high activity sinogram, which comprise true, random and scatter events. The total count rate R_T is obtained by dividing the total counts by the duration of acquisition. As in scatter fraction experiment, the low activity data are used to calculate the scatter fraction SF_i and the true count rate R_{true} for each slice (Eqs. 5.7 and 5.8). The random count rate R_r for each slice is then calculated by (Daube-Witherspoon et al., 2002)

$$R_r = R_T - [R_{true} / (1 - SF_i)] \tag{5.10}$$

The system random count rate is calculated by summing R_r values for all slices.

The noise equivalent count rate (*NECR*) for each slice is computed by Eq. (5.4) as

$$NECR = (R_{true})^2 / R_T \tag{5.11}$$

The system *NECR* is computed as the sum of all *NECR*s over all slices.

The percent dead time count loss ($\%DT$) as function of activity is calculated by

$$\%DT = (1 - R/R_{extrap}) \times 100 \tag{5.12}$$

where R_{extrap} is the count rate extrapolated from the low activity data to the time when the total count rate R_T is measured, and R is the true count rate (equal to R_T corrected for scatter and random events).

Questions

1. The typical transaxial resolution at 1 cm of a PET scanner ranges between (A) 14 and 16 mm (B) 3 and 4 cm (C) 4 and 7 mm.
2. What are the common factors that affect the spatial resolution of a PET scanner? Out of these, which one is most predominant?
3. The transverse resolution is worse at the center of the FOV than away from the center. True _____; False _____.
4. The axial resolution of a scanner is its ability to differentiate two points on an image along the axis of the scanner. True _____; False _____.
5. If the detector size is 8 mm, what is the expected approximate spatial resolution for ^{18}F-FDG PET images at the center of the FOV?
6. The maximum positron energy for ^{18}F is 0.64 MeV and for ^{82}Rb is 3.35 MeV. Which radiopharmaceutical would provide better spatial resolution?
7. Non-colinearity is a factor that affects the spatial resolution of a PET scanner. How is it affected by the diameter of the detector ring? For a 90 cm diameter detector ring, what is the value of the non-colinearity component in the overall spatial resolution?
8. Describe the method of measuring transverse radial, transverse tangential, and axial spatial resolutions of a PET scanner.
9. Define the sensitivity of a PET scanner and discuss the important parameters that affect the sensitivity.
10. Scanner 1 has twice the ring diameter of scanner 2. The ratio of sensitivities of scanner 1 to scanner 2 is:
    (A) 0.75
    (B) 0.67
    (C) 0.25
11. The sensitivity in 3-D acquisition is 4 to 8 times higher than in 2-D acquisition. Why?
12. The overall sensitivities of PET scanners in 2-D mode are:
    (a) 1 to 2%
    (b) 3 to 5%
    (c) 0.2 to 0.5%

and in 3-D mode:
(a) 20 to 30%
(b) 2 to 10%
(c) 35 to 45%

13. Scanner 1 has the detectors of size 3 mm, and scanner 2 has the detectors of size 6 mm. Assuming that all detectors are squares and all other parameters are the same, the sensitivity of scanner 1 is: (A) half; (B) one-tenth; or (C) one-fourth of scanner 2.
14. Describe the methods of daily and weekly quality control tests.
15. Explain why and how normalization of PET acquisition data is carried out.
16. What are acceptance tests? Describe the methods of determining sensitivity and scatter fraction for a PET scanner.
17. The noise equivalent count rate (*NECR*) is proportional to the signal-to-noise in the reconstructed image. True _____; False _____.
18. The sensitivity of a scanner increases with (A) the size of the detector in the ring True _____; False _____; (B) with the diameter of the detector ring True _____; False _____.
19. Scanner 1 has the individual detector size of 36 mm^2 and scanner 2 has the detector size of 60 mm^2. Scanner 1 has (A) 30%; (B) 60%; (C) 1.7 times the sensitivity of scanner 2.
20. Define contrast of an image. Elucidate the different factors that affect the contrast.

References and Suggested Reading

1. Budinger TF. PET instrumentation: what are the limits? *Semin Nucl Med.* 1998;28:247.
2. Brix G, Zaers J, Adam LE, et al. Performance evaluation of a whole-body PET scanner using the NEMA protocol. *J Nucl Med.* 1997;38:1614.
3. Buchert R, Bohuslavizki UH, Mester J, et al. Quality assurance in PET: Evaluation of the clinical relevance of detector defects. *J Nucl Med.* 1999; 40:1657.
4. Daube-Witherspoon ME, Karp JS, Casey ME, et al. PET performance measurement using the NEMA NU 2-2001 standard. *J Nucl Med.* 2002;43:1398.
5. Huesman RH. The effects of a finite number of projection angles and finite lateral sampling of projections on the propagation of statistical errors in transverse section reconstruction. *Phys Med Biol.* 1977;22:511.
6. Karp JS, Daube-Witherspoon ME, Hoffman EJ, et al. Performance standards in positron emission tomography. *J Nucl Med.* 1991;32:2342.
7. Kearfott K. Sinograms and diagnostic tools for the quality assurance of a positron emission tomograph. *J Nucl Med Technol.* 1989;17:83.
8. Keim P. An overview of PET quality assurance procedures: Part 1. *J Nucl Med Technol.* 1994;22:27.
9. Moses WW, Derenzo SE. Empirical observation of performance degradation in positron emission tomographs utilizing block detectors. *J Nucl Med.* 1993; 34:101P.

10. National Electrical Manufacturers Association. NEMA Standards Publications NU 2-1994. *Performance Measurements of Positron Emission Tomographs.* Washington DC: National Electrical Manufacturers Association; 1994.
11. National Electrical Manufacturers Association. NEMA Standard Publication NU 2-2001. *Performance Measurements of Positron Emission Tomographs.* Rosslyn, VA: National Electrical Manufacturers Association; 2001.
12. Tarantola G, Zito F, Gerundini P. PET instrumentation and reconstruction algorithms in whole-body applications. J Nucl Med 2003;44:756.